International Journal of Mechanical Engineering and Robotics Research

ISSN 2278 – 0149 www.ijmerr.com
Vol. 3, No. 2, April, 2014


*Research Paper*

# FINITE ELEMENT ANALYSIS OF HOT ROLLING OF STRUCTURAL STEEL

**Yellappa M[1]*, Satyamurthy N[2], Uday M[1], Giriswamy B G[1] and Puneet U[1]**

**Corresponding Author:* ***Yellappa M,*** ✉ *meetyellappa1983@gmail.com*

The rolling process is one of the most popular processes in manufacturing industries, such that almost 80 percent of metallic equipment has been exposed to rolling at least one time in their production period. Among all kinds of rolling processes, at rolling is the most practical. In industrial countries, about 40-60 percent of rolling products are produced with this type of rolling. Throughout this century, the rolling process has been analyzed by various analytical and numerical methods such as the slab method, the slip-line field method, the upper bound method, the boundary element method and the finite element method. The hot rolling process to form I or H section beam is simulated statically using rezoning. The software used is ANSYS v14.0. The static analysis is performed in two load steps: the first builds up the rolling process, and hot rolling occurs in the second. In the first load step, the billet moves toward rigid rollers to establish contact with the rollers and to fill the gap between the rollers. In this present work, the simulation terminates at near the end of the first load step due to mesh distortion. A rezoning operation repairs the distorted mesh, and the analysis resumes and continues to completion using the new mesh. The parameters such as residual stress, effective plastic strain region, metal flow, temperature distribution, moment of top roller & reaction are being simulated and being represented graphically..

***Keywords:*** Hot rolling, Finite Element Methods, Static analysis, Plastic strain region, Residual stress.

## INTRODUCTION

Metal rolling is one of the most important manufacturing processes in the modern world. The large majority of all metal products produced today are subject to metal rolling at one point in their manufacture. Metal rolling is often the first step in creating raw metal forms. The inot or continuous casting is hot rolled into a bloom or a slab; these are the basic structures for the creation of a wide range of manufactured forms. Blooms typically have a square cross section of greater than 6x6 inches. Slabs are rectangular and are usually greater than 10 inches in width and more than 1.5 inches in thickness. Rolling is most often, (particularly in the case of the conversion of an ingot or continuous casting), performed hot.

[1] Assistant Professor, Mechanical Department, SJBIT, Bangalore-60, India.

[2] Associate Professor, Mechanical Department, SJBIT, Bangalore-60, India.

Blooms and slabs are further rolled down to intermediate parts such as plate, sheet, strip, coil, billets, bars and rods. Many of these products will be the starting material for subsequent manufacturing operations such as forging, sheet metal working, wire drawing, extrusion, and machining. Blooms are often rolled directly into I beams, H beams, channel beams, and T sections for structural applications. Rolled bar of various shapes and special cross sections is used in the machine building industry, as well as for construction. Rails, for the production of railroad track are rolled directly from blooms.

Plates and sheets are rolled from slab, and are extremely important in the production of a wide range of manufactured items. Plates are generally considered to be over 1/4", (6mm), in thickness. Plates are used in heavy applications like boilers, bridges, nuclear vessels, large machines, tanks, and ships. Sheet is used for the production of car bodies, buses, train cars, airplane fuselages, refrigerators, washers, dryers, other household appliances, office equipment, containers, and beverage cans, to name a few. It is important to understand the significance of metal rolling in industry today, as well as its integration with other manufacturing processes.

## METAL ROLLING PRINCIPLES

Most metal rolling operations are similar in that the work material is plastically deformed by compressive forces between two constantly spinning rolls. These forces act to reduce the thickness of the metal and effect its grain structure. The reduction in thickness can be measured by the difference in thickness before and after the reduction, this value is called the draft. In addition to reducing the thickness of the work, the rolls also act to feed the material as they spin in opposite directions to each other. Friction is therefore a necessary part of the rolling operation, but too much friction can be detrimental for a variety of reasons. It is essential that in a metal rolling process the level of friction between the rolls and work material is controlled, lubricants can help with this. A basic flat rolling operation is shown in figure 1.1; this manufacturing process is being used to reduce the thickness of a work piece.

**Figure 1: Basic Flat Rolling Operation**

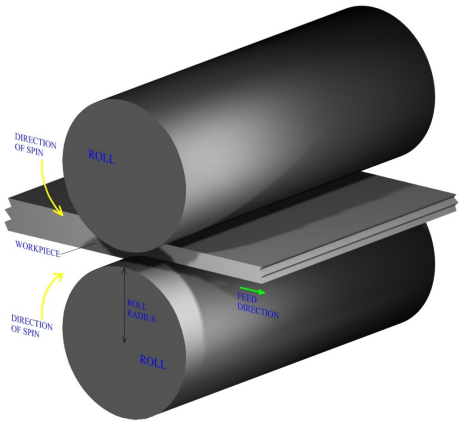


During a metal forming operation, the geometric shape of the work is changed but its volume remains essentially the same. The roll zone is the area over which the rolls act on the material, it is here that plastic deformation of the work occurs. An important factor in metal rolling is, that due to the conservation of the volume of the material with the reduction in thickness, the metal exiting the roll zone will be moving faster than the metal entering the roll zone. The rolls themselves rotate at a constant speed, hence at some point in the roll zone the surface velocity of the rolls and that of the material are exactly the same. This is termed the no slip point.Before this point the rolls are moving faster than the material, after this point the material is moving faster than the rolls.

**Figure 2: No Slip Point in Rolling**

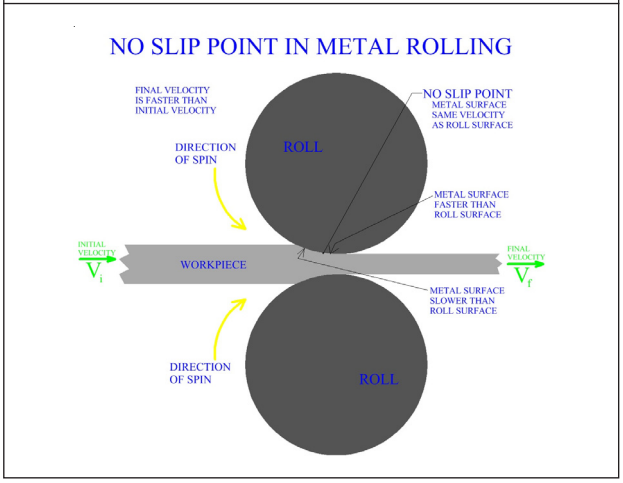


## ROLLS FOR FORMING

Metal rolling operations can produce a wide range of different formed products. The width of rolled work can be as much as several meters, or narrower than a thousandth of an inch. Metal forming manufacture also creates rolled work over a wide range of thicknesses. Metal plates for some boilers may be rolled to a thickness of 12 inches, while foil for wrapping cigarettes and candy can be .0003 inches thick. Rolls used in metal forming are of various sizes and geometries. In flat rolling industrial manufacture, the rolls may typically be 24 to 54 inches in diameter. In some rolling operations, in the forming of very thin work, the rolls can be as small as 1/4 inch.

Rolls are subject to extreme operating conditions including, tremendous forces, bending moments, thermal stresses, and wear. Roll materials are selected for strength, rigidity, and wear resistance. Roll materials vary dependent upon the specific forming process. Common roll materials are cast iron, cast steel, and forged steel. Forged rolls are stronger and more rigid than cast rolls but are more difficult to manufacture. In some industrial forming processes rolls are made from nickel steel or molybdenum steel alloys. With metal rolling operations of certain materials, rolls made of tungsten carbide can provide extreme resistance to deflection.

## ROLL DEFLECTIONS

Strength and rigidity are important characteristics of the rolls used to form product in metal rolling manufacture. The particular attributes of the rolls will effect dimensional accuracy as well as other factors in the operation. During the rolling process great forces act upon the rolls. Rolls will be subject to different degrees of deflection. In any particular rolling process, it is important to understand how these deflections will effect the rolls and hence the work being formed. The rolls initially start out flat. During a basic flat rolling operation, it can be observed that the work material will exert greater force on the rolls towards the center of the material than at its edges. This will cause the rolls to deflect more at the center, and hence gives the work a greater thickness in the middle.

**Figure 3: Roll Deflections**

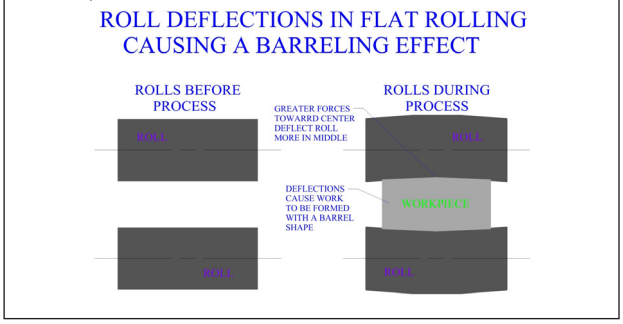


## DEFECTS IN METAL ROLLING

A wide variety of defects are possible in metal rolling manufacture. Surface defects commonly occur due to impurities in the material, scale, rust, or dirt. Adequate surface preparation prior to the metal rolling operation can help avoid these. Most serious internal defects are caused by improper material distribution in the final product. Defects such

as edge cracks, center cracks, and wavy edges, are all common when metal forming by this method.

**Figure 4: Rolling Defects**

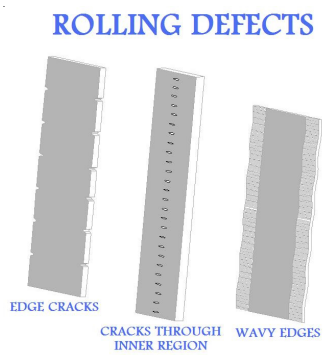


Often times a sheet is not defective, it is just not flat enough. In sheet metal industrial practice, a sheet may be passed through a series of leveling rolls that flex the sheet in opposite directions to flatten it. Another interesting defect that can occur in flat rolling is alligatoring, where the work being rolled actually splits in two during the process. The two parts of the work material travel in opposite directions relative to their respective rolls.

## A36 STRUCTURAL STEEL

A36 steel is a standard steel alloy which is a common structural steel used in the United States. The A36 standard was established by the standards organization ASTM International. A36 is a standard low carbon steel, without advanced alloying.A steel may be classified as a carbon steel if (1) the maximum content specified for alloying elements does not exceed the following: manganese-1.65%, silicon-0.60%, copper-0.60%; (2) The specified minimum for copper does not exceed 0.40%; and (3) no minimum content is specified for other elements added to obtain a desired alloying effect.

## HOT ROLLING PROCESS

### Description of the Hot-Rolling Process

The hot-rolling process consists of two primary phases, unsteady and steady. The starting and the ending of the hot-rolling process represent the unsteady phase, while the rest of the process represents the steady-state phase. In the unsteady phase, the billet (rectangular bar of steel) comes into contact with the rollers and fills the gap between the rollers before moving through the rollers. When the billet begins to move through the rollers, the process is considered to be in a steady state until the end face of the billet comes into contact with the rollers.

### Hot Rolling Process Simulation

Although a transient analysis is often used to simulate the hot-rolling process, a static analysis is generally preferred when dynamic effects are unimportant or when a transient analysis may require excessive resources. This example shows how both the unsteady and steady phases of the hot-rolling process can be simulated via a static analysis.

The static analysis is performed in two load steps: the first builds up the rolling process, and hot rolling occurs in the second.In the first load step, the billet moves toward rigid rollers to establish contact with the rollers and to fill the gap between the rollers. In order to build up the rolling process, the billet should partially fill the gap between rollers so that when rollers begin to rotate, they can pull the billet in via friction. In the second load step, the rollers pull the billet in and eventually shape the rectangular billet into an I-section block.In this present work the simulation terminates at near the end of the first load step due to mesh distortion. A rezoning operation repairs the distorted mesh, and the

analysis resumes and continues to completion using the new mesh.

## Problem Description

A rectangular block is passed through set of rollers to obtain an I-shaped beam, as shown in the following figure.

**Figure 5: Hot Rolling Model**

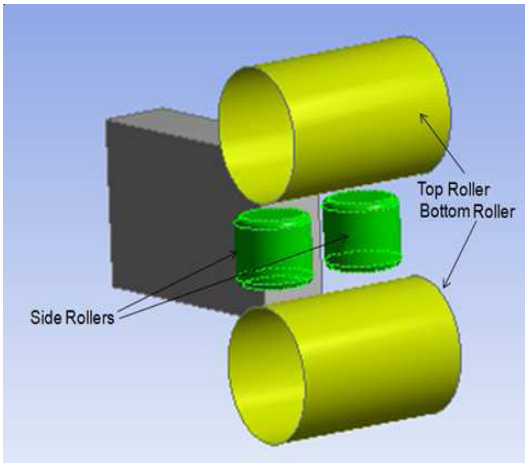


## Top and Bottom Rollers

Horizontal cylindrical rollers pull the block from the top and bottom to increase the width andreduce the depth of the block. The rollers control the width of the flange parts of the I-shape;they are modeled using rigid target elements.

## Side Rollers

Vertical cylindrical rollers with small fillets at either end. The fillets are necessary to ensure smooth material flow. The side rollers pull the block from the sides to create the I-shaped cross section. They control the width of the web part of the I-shape. As with the top and bottom rollers, the side rollers are modeled using rigid target elements. The following figure shows that the problem is symmetrical about two planes (XZ and YZ).

**Figure 6: Symmetric Hot Rolling Modeling**

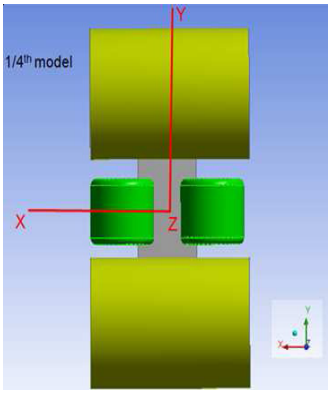


To reduce modeling and computational time, therefore, only one quarter of the model is analyzed. After the analysis has completed, however, the results are viewable in the full model by performing symmetry expansion about two planes of symmetry.

The simulation is performed statically in two load steps. In the first load step, the block is moved towards fully constrained rigid rollers in order to build up the rolling process. In the second load step, hot-rolling is performed by rotating the rollers about their axes of rotation, and the block is free to move in the horizontal direction (Z).

As the rollers rotate, the block passes through them due to the high level of friction between the rollers and the block. Eventually, the full block passes through the rollers to achieve the I-shaped cross section. In such large-deformation problems, however, mesh distortion is common, leading to convergence difficulties or eventual analysis termination. The analysis diverges in the first load step due to excessive distortion in a few elements. A rezoning operation repairs the distorted mesh and allows the analysis to continue.

## Modeling

The following figure shows one-quarter of the model all that is necessary for this analysis:

**Figure 7: Hot Rolling Quarter Model Geometry**

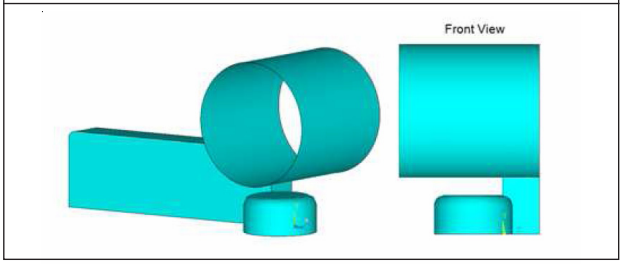


The geometry of the block is 1/4 of the full geometry of the block shown in the above Figure.

Appropriate geometries for the rollers are also considered in the quarter model. This problem is symmetric about a plane when the flow on one side of the plane is a mirror image of flow on the opposite side. By definition, a symmetry boundary condition refers to a planar boundary surface. In this case, the physical problem has four-way symmetry. The computational domain can therefore be limited to one quarter of the duct, using two Symmetry Plane boundaries. In this problem we have two surfaces that meet at a sharp angle, and both are symmetry planes, so we can set each surface to be a separate named boundary condition, rather than combine them into a single one. Thus, we can position your model so that symmetry planes are perpendicular to coordinate axes if possible. This improves the performance of the CFX-Solver.

Use of the symmetry specification has two distinct advantages:

(1) To save the user modeling 1/2 or 3/4 of the structure

If the SYMX data record (only) is used, only half of the structure needs to be defined (on one side of the x axis). The other half of the structure will be generated internally by the program as a mirror image of the first half about the x axis. If the whole structure is modeled, the SYMX data record must not be used as this produces two identical structures existing in the same position.

If the SYMY data record (only) is used, only half of the structure needs to be defined (on one side of the y axis). The other half of the structure will be generated internally by the program as a mirror image of the first half about the y axis. If the whole structure is modeled the SYMY data record must not be used as this produces two identical structures existing in the same position.

If both the SYMX data record and SYMY data record are used, only one quarter of the structure needs to be defined (in one quadrant). If the half/whole structure is modeled both data records must not be used as this produces identical structures existing in the same position.

(2) To save substantial computer time in the radiation/diffraction analysis in AQWA-LINE

**Expected saving in computer time:**

for 2-fold symmetry (SYMX OR SYMY) = 50 - 75 percent

for 4-fold symmetry (SYMX and SYMY) = 75 - 90 percent

These figures given are typical and saving will be model dependent. Saving may be less for small problems, and should be even greater for very large problems, i.e. greater than 250 defined (as opposed to total) elements.

## Modeling The Block

**Figure 8: Meshed Model With Dimensions**

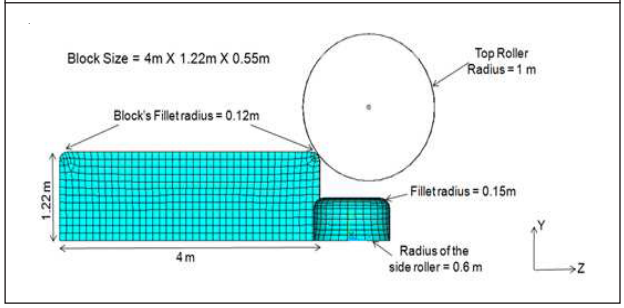

## Contact Modeling

The following two contact pairs are created:

- Contact Pair between Block and Top Roller
- Contact between Block and Side Roller

Contact Pair between Block and Top Roller

**Figure 9: Contact between Block and Top Roller**

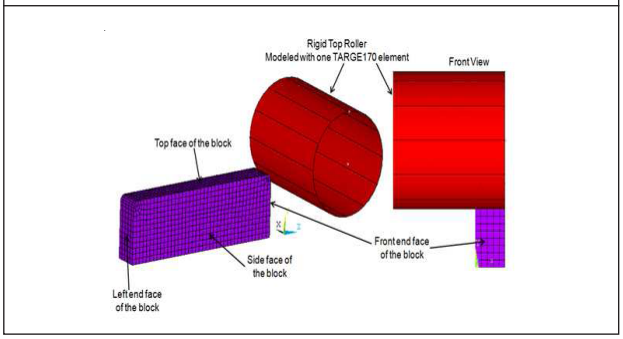


**Figure 10: Contact Between Upper and Lower Rollers With Workpiece**

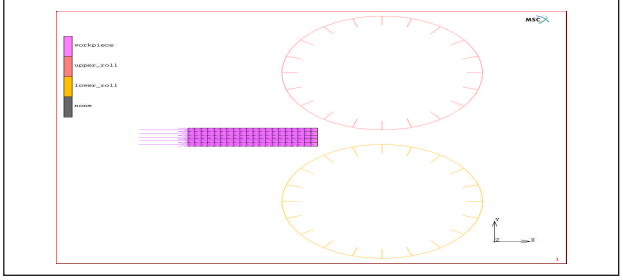

## Contact between Block and Side Roller

A standard rigid-flexible contact pair is created between the side roller and the block. As shown in the following figure, the contact pair is created between two faces (front and side faces) of the
block and side rollers:

**Figure 11: Contact between Block and Side Roller**

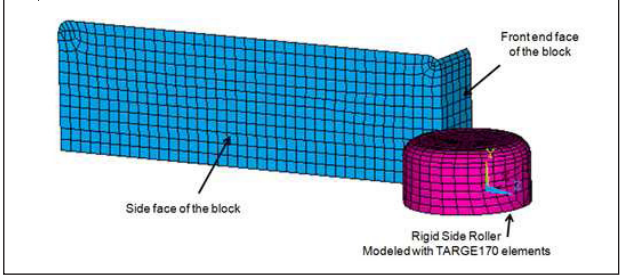


# BOUNDARY CONDITIONS & LOADINGS

Symmetric boundary conditions are applied on both symmetry planes of the block, as shown in the following figure.

**Figure 12: Boundary Conditions Imposed on Bar**

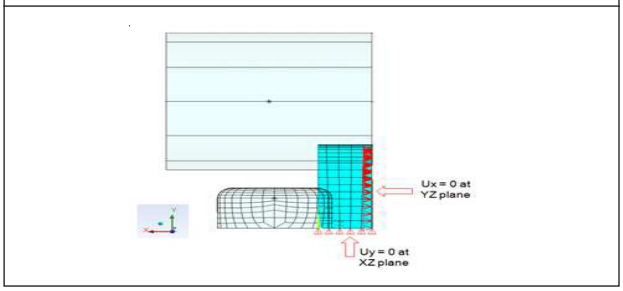


(1) The top & the bottom rollers restricts the movement of the structural steel bar in Y direction i.eUy=0.

(2) The two horizontal side rollers restricts the movement of the structural steel bar in X direction i.eUx=0.

To showcase the usefulness of rezoning in 3-D problems, this problem is solved statically in two load steps:

- Load Step 1: Establish Contact with Rollers
- Load Step 2: Hot-Rolling

**Load Step 1:** Establish Contact with Rollers The block is allowed to move towards the rollers and establish contact with them. Thedisplacement (Uz = 1.5 m) is applied on the left end face of the block, as shown in the following figure:

**Figure 13: Load Step 1: Establish Contact with Rollers**

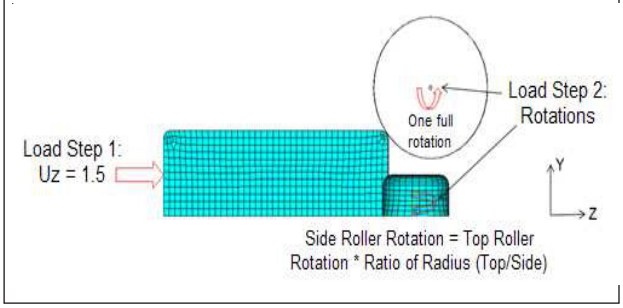

Both the rigid rollers (top and side) are constrained in all directions with the use of pilot nodes. No friction is used.

```
!Load Step 1
!Boundary Conditions
cmsel,s,ux_node          ! Select node on symmetry plane (YZ plane)
d,all,ux                      ! Apply symmetry boundary conditions
cmsel,s,uy_node          ! Select node on symmetry plane (XZ plane)
d,all,uy                      ! Apply symmetry boundary conditions
d,9999,all          ! Constrain top roller in all degrees of freedom
d,20999,all         ! Constrain side roller in all degrees of freedom
allsel,all
! Loadings
cmsel,s,uz_node     ! Select the nodes of the left end face of the block
d,all,uz,1.5        ! Apply prescribed displacement (Uz =1.5m)
mp,mu,1,0           ! Use zero value of friction
```

### Load Step 2: Hot-Rolling

Hot-rolling occurs in this load step. The rollers are allowed to rotate, and the block is free to move in the Z direction. A high value of friction ($\mu$ = 0.6) is used.Because the top and side rollers are different sizes, different rotations are given to the rollers in order to maintain continuity. Based on the size of top roller, the friction coefficient, and the block length, one full rotation is applied to the top roller. No forward or backward slip is considered while calculating the rotation value of the side roller. Rotation of the side roller is calculated using this formula:

Rotation of side roller = Rotation of top roller * (Radius of top roller / Radius of side roller)

## ANALYSIS & SOLUTION CONTROL

A nonlinear static analysis is performed in two load steps of one second each. The analysis diverges in the first load step, rezoning occurs, and the analysis resumes.

Restart files are saved at each sub step, as rezoning requires a restart file, and the sub step at which rezoning is required is still unknown. Results items are also stored at each sub step. Restart files and results items are saved at each and every substep,despite the considerable memory requirements for doing so. In most cases, it is sufficient to save them at every few sub steps instead.The initial run diverges in the first load step at TIME = .7718.

The following figure shows the deformed shape of the model at the last converged substep i.e. at 40$^{th}$ substep.

**Figure 14: Deformation in the First Load Step at 40$^{th}$ Substep**

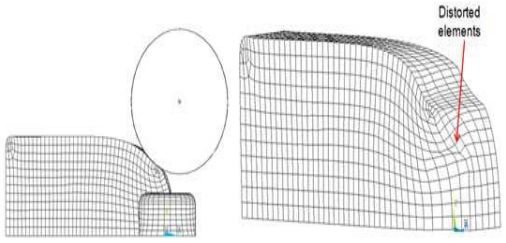


Element shape checking of the deformed model suggests that the mesh is overly distorted at thelocation indicated.

Rezoning repairs the distorted mesh and allows the analysis to continue. Rezoning is applied tothis problem as described:

- Rezoning Initiated at the 30th Substep
- Distorted Mesh Replaced by an Imported New Mesh
- Solution Items Mapped from Original Mesh to New Mesh
- Analysis Resumes Using the New Mesh

The rezoning process involves the following general tasks:

1) Determine the load step and substep at which the region must be remeshed
2) Initiate the rezoning process.
3) Select the region to remesh.
4) Remesh the region with a mesh of better quality than the distorted mesh in the original domain.
5) Verify boundary conditions, loads, temperatures, and fluid-penetration parameters applied to the new mesh (from the old, distorted mesh).
6) Automatically map displacements and state variables from the old (distorted) mesh to the new mesh and rebalance the resulting residual forces

7) Use the restart capability to continue the analysis.

## Rezoning Initiated at the 30th Substep

The best substep at which to initiate rezoning is determined by examining the deformed model and the physics of the simulation. The analysis diverges after the 40th substep at TIME = .7718. Very little time (from TIME = .77 to .7718) occurs between the 31st to the 40th substeps, however, indicating that severe distortion of the mesh begins to occur at the 31st substep. Because rezoning should be attempted at one or more substeps before the substep where mesh deformation occurs, the 30th substep is a logical choice at which to initiate rezoning. Shapechecking (SHPP or CHECK) of the deformed mesh at the 30th substep confirms the choice, as the deformed mesh violates no error limits.

The following figure shows the deformed mesh at the 30th substep:

**Figure 15: Deformed Mesh**

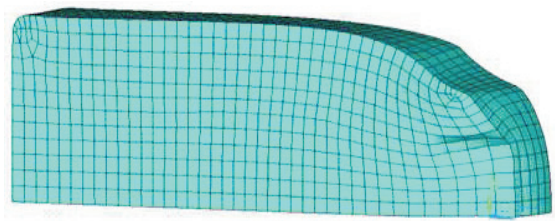

**Figure 16: Distorted Mesh Replaced by an Imported New Mesh**

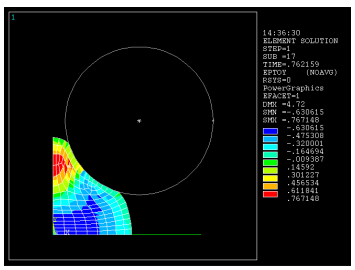

Various remeshing options are available for rezoning. Because this is a 3-D problem, however, a new mesh is read in to replace the original, distorted mesh. The new mesh can be generated in Workbench or by other third-party software by first creating the deformed geometry from the deformed mesh, then meshing the deformed geometry with new settings to obtain a new, good mesh. The new mesh must be better than the original mesh; otherwise, rezoning cannot improve convergence.

In this work, new mesh is generated in Workbench using the BrepUpdaterfeature. The following figure shows original, deformed mesh and the new, good mesh:

Various remeshing options are available for rezoning. Because this is a 3-D problem, however, a new mesh is read in to replace the original, distorted mesh. The new mesh can be generated in Workbench or by other third-party software by first creating the deformed geometry from the deformed mesh, then meshing the deformed geometry with new settings to obtain a new, good mesh. The new mesh must be better than the original mesh; otherwise, rezoning cannot improve convergence.

In this work, new mesh is generated in Workbench using the BrepUpdaterfeature. The following figure shows original, deformed mesh and the new, good mesh.

**Figure 17: Deformed Mesh & New Mesh After Rezoning**

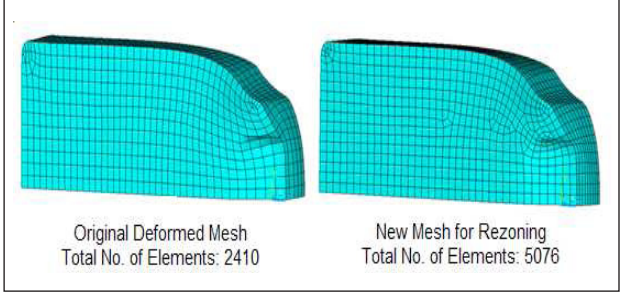

The following input initiates rezoning at the 30th substep and reads in the new mesh.

```
/solu
rezone,manual,1,30          ! Start rezoning at the 30th substep
remesh,start                          ! Start "remeshing" process
remesh,read,Rezone_Mesh,cdb       ! Read new mesh in "cdb" format
remesh,finish                          ! Transfer boundary conditons and loadings from the
!                                  old mesh to the new mesh, and recreate contact
!                                  pairs (if any)
```

After remeshing (REMESH,FINISH), the program transfers surface loads, forces, boundary conditions, and contact pairs (if any) from the original, deformed old mesh to the new, good mesh. It is good practice to check the model after remeshing to verify that all such transfers to the new mesh were successful.

Solution Items Mapped from Original Mesh to New Mesh

After remeshing, solution and results items from the original mesh are mapped to the new mesh, and the resulting residual forces are rebalanced (MAPSOLVE). The mapping operation concludes the rezoning process, and a standard multiframe restart resumes solution processing using the new mesh.

Analysis Resumes Using the New Mesh After mapping quantities from the old to the new mesh and rebalancing the residual forces, a multiframe restart (ANTYPE,, RESTART,,, CONTINUE) resumes the nonlinear solution with the new mesh.

The following input restarts the analysis:

```
/clear,nostart
/file,Hot_Rolling_Model    ! Give same job name as initial run
/solu
antype,,restart,1,30              ! Specify analysis type (restart), load step, and substep
solve                      ! Solve first load step

! Load Step2: Rotate rollers
time,2                     ! Define time for second load step
esel,s,ename,,185
allsel,below,element       ! Select the nodes of the block
ddel,all,uz                      ! Free the block to move in Z direction
allsel,all
nsel,s,,,9999
d,all,rotx,-6.28            ! Rotate top roller
nsel,s,,,20999
d,all,roty,-10.47          ! Rotate side roller
allsel,all
mp,mu,1,0.6                      ! Use high value of friction
OUTRES,ALL,10               ! Save results items at every 10th substep
RESCONTRL,DEFINE,ALL,30,0   ! Save restart files at every 30th substep
NSUBST,1000,100000,20
solve                       ! Solve second load step
```

## RECOMMENDATIONS

To perform a similar 3-D simulation using rezoning, consider the following hints and recommendations:

(1) The hot-rolling process can be simulated via static analysis in two load steps. The first load step pushes the billet until it establishes contact with the rollers, and the second pulls the billet by rotating the rollers.

(2) Before rezoning, back up results and restart files associated with the initial run in a separate directory. Rezoning updates results and restart files, so the original files are no longer available shoul to try rezoning at another substep.

(3) If rezoning is performed at a substep where the original mesh is too distorted (where shape-checking [SHPP or CHECK] indicates errors), then rezoning will not work. Rezoning should therefore be performed at an earlier substep.

(4) A new mesh that is too fine as compared to the original mesh may cause mapping (MAPSOLVE) errors. The primary requirement for the new mesh is that it should properly capture the outer surface geometry of the deformed model.

## RESULTS AND DISCUSSIONS

**Table 1: Constituents of the A36 Structural Steel Beam**

| Elements | C | Si | Mn | P | S | Ni | Cr | Cu |
|---|---|---|---|---|---|---|---|---|
| % | 0.14 | 0.35 | 0.052 | 0.024 | 0.21 | 0.18 | 0.18 | 0.23 |

**Table 2: Mechanical & Thermal Properties of A36 Beam**

| | |
|---|---|
| Density | 7800 kg/m3 |
| Young's Modulus | 290 GPa |
| Poisson's ratio | 0.3 |
| Shear Modulus | 79.3 GPa |
| Ultimate Yield Strength | 400-500 Mpa |
| Thermal Conductivity | 143.4 W/m/k |
| Tangent Modulus | 2 GPa |
| Coefficient of friction | 0.6 |

| Table 3: Dimensions of the A36 Rectangular Beam | |
|---|---|
| Length | 4 m |
| Width | 0.55 m |
| Height | 1.22 m |
| Fillet Radius | 0.12 m |

| Table 4: Dimensions of the Work Roll | |
|---|---|
| Radius of the vertical rollers | 1 m |
| Radius of the horizontal rollers | 0.6 m |
| Speed of the vertical rollers | 9.869 m/sec |
| Speed of the side rollers | 47.123 m/sec |
| Fillet radius of the horizontal rollers | 0.15 m |

| Table 5: Thermal Properties of the Work Roll | |
|---|---|
| Heat capacity | 460 J/kg/k |
| Thermal Conductivity | 14 W/m/k |
| Density | 7800 Kg/m3 |

## DEFORMATION PLOT

The following figure shows the deformation plot against the cross section of the beam (USUM) of the initial run at the last converged substep (TIME = .7718)

**Figure 18: USUM Plots: Initial Run at Last Converged Substep**

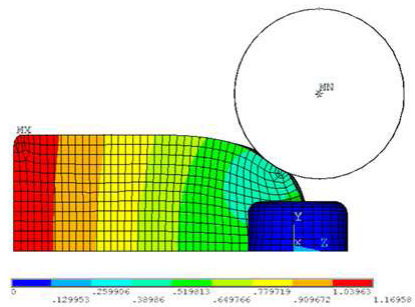

Following the successful rezoning, the following figure shows the deformation plot (USUM) of the model after building up the rolling process (at the end of the first load step):

**Figure 19: USUM Plots: After Building Up the Rolling Process**

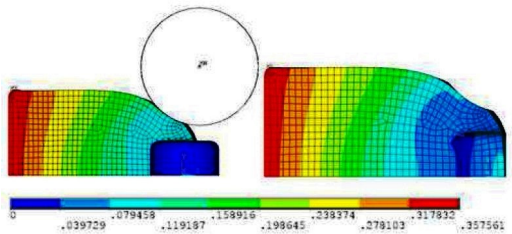

The hot-rolling process is performed in the second load step by rotating the rollers and using high friction contact between the rollers and the billet. The following figure shows the deformation plot (USUM) of the model at the end of the second load step.

**Figure 20: USUM Plots: After End of Rolling Process**

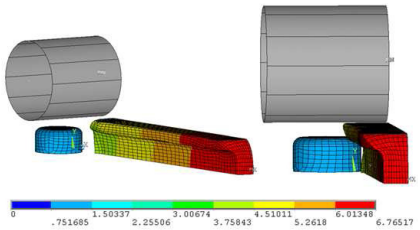

To view the full-model results, two symmetric expansions (/EXPAND) are performed. The following input performs the symmetric expansion:

```
cs, 11, 0, 28752, 29076, 28734,1,1 ! Create local Cartesian coordinate system (using
YZ symmetry plane of the block

/EXPAND, 1, LRECT, HALF, , .000001,,1, LRECT, HALF,,,.000001, ,RECT, FULL
```

The following figure shows the deformation plot in the fully expanded model, where therectangular block becomes an I-shaped beam:

**Figure 21: USUM Plot of Full Model after Symmetry Expansion**

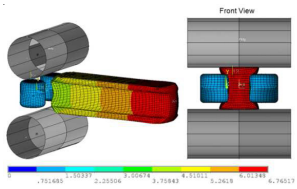

**Table 6: Contact Pressure During Hot Rolling Process**

| Time ( sec) | Experimental data (N/mm2) | FEA data (N/mm2) |
|---|---|---|
| 0.07 | 22912.2 | 2491.68 |
| 0.10 | 2319.2 | 2491.68 |
| 0.15 | 2348.48 | 2491.68 |
| 0.20 | 2434.4 | 2491.68 |
| 0.25 | 2477.12 | 2491.68 |

So from the above result it is quite clear that the experimental data and FEA data are in good agreement with a percentage error of 4.8%.

## DEFORMATION ANIMATION

**Figure 22: Deformation (USUM) in the Initial Run**

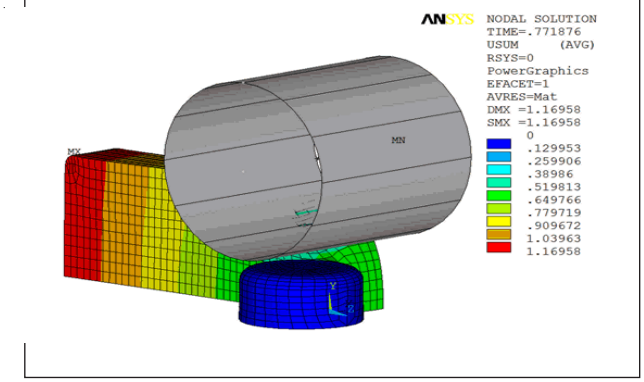


## DEFORMATION ANIMATION

**Figure 23: Deformation (USUM) after rolling process**

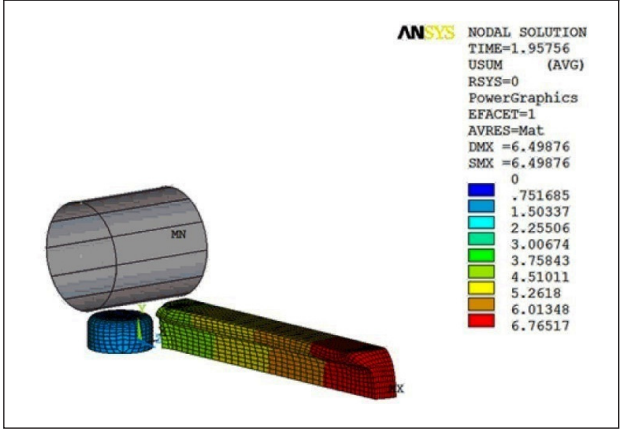


**Figure 24: Deformation (USUM) After Rezoning in the Expanded Model**

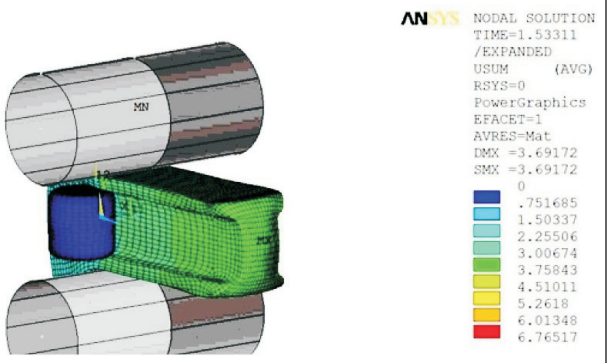


## RECOMMENDATIONS

To perform a similar 3-D simulation using rezoning, consider the following hints and recommendations:

(1) The hot-rolling process can be simulated via static analysis in two load steps. The first load step pushes the billet until it establishes contact with the rollers, and the second pulls the billet by rotating the rollers.

(2) Before rezoning, back up results and restart files associated with the initial run in a separate directory. Rezoning updates results and restart files, so the original files are no longer available shoul to try rezoning at another substep.

(3) If rezoning is performed at a substep where the original mesh is too distorted (where shape-checking [SHPP or CHECK] indicates errors), then rezoning will not work. Rezoning should therefore be performed at an earlier substep.

(4) A new mesh that is too fine as compared to the original mesh may cause mapping (MAPSOLVE) errors. The primary requirement for the new mesh is that it should properly capture the outer surface geometry of the deformed model.

(5) Check the model after remeshing (REMESH,FINISH) to verify that all boundary conditions, contact pairs, and loadings have transferred correctly from the original mesh to the new mesh.

(6) After rezoning, if the analysis diverges again after passing the initial run's diverged time, multiple rezonings may be necessary. If the analysis diverges again before passing the initial run's diverged time, then either the new mesh is of insufficient quality, or other problems unrelated to mesh distortion (such as geometry and material instabilities) exist.

Equivalent Plastic Strain Plot in the Full Expanded Model

**Figure 25: Equivalent Plastic Strain Plot in the Full Expanded Model**

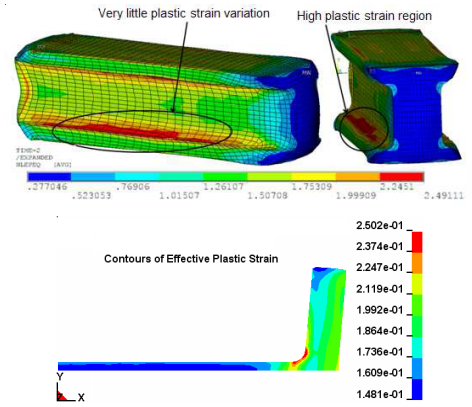


**Figure 26: Stress Contour in the Pressing Direction of Horizontal Roller**

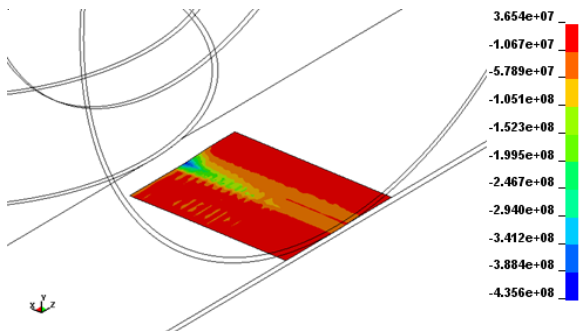


Based on the simulation of the H-Beam rolling process, we can obtain the distribution and change of stress and strain in different passes as well as under different forming situation at all spots and time. We can justify the forming status and the force distribution, which benefits the design of rolling grooves, from every part of the work piece by the outcome of structure simulation. Figure 4.6 is the strain field of the large H-Beam quarter section. It is quite clear that the connection area of the flange and web experiences highest strain during rolling.For some duration in the rolling process, the plastic strain varies little over time in the high plastic strain region. This behavior occurs during the steady-state (rolling) phase of the simulation. Figure 4.7 is the stress contour in the pressing direction of horizontal roller during the rolling process, which shows that the highest stress is located in the connection area of flange and web during rolling. The reason for this is because at the area at intersection of web and flange there is sudden change in cross section area.

**Figure 27: Effective Strain v/s Thickness of I Beam**

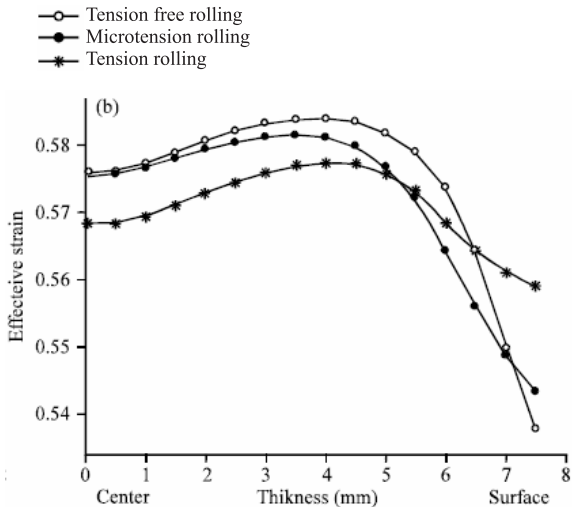

The above fig shows variation effective strain rate with respect to the thickness of I beam cross section. This fig was published in Inform Technol Journal 10-12 2406-2412 the analysis of hot rolling of I beam in the year 2010. Thus, it is evident from the that the maximun effective strain or the plastic region exist in between the centre and the surface of the I beam which is the area connecting web and flange. Hence, the simulation is somewhat close to the published data.

## METAL FLOW SIMULATION

**Figure 28: Vector of metal flow in the I-Beam section ?X Groove?**

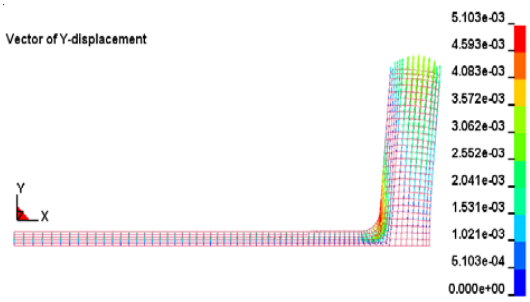


During the rolling of the H-beam, the status of metal flow in different parts determines final shape and dimension of the product. We can directly instruct the design of the grooves and process by simulation results. Figure 4.3 shows the displacement vector of the metal flow in the flange stretching direction (y direction) during rolling. It can be easily concluded that the outer side of the flange flows toward top of the flange and the inner side of the flange flows toward the connection area of flange and web which is flow along the curve of horizontal roller. This reverse phenomenon shows that as an integrated work piece there is some sort of metal flow in the section of the H-beam in order to make up the difference of the stretching between the web and flange.

## TEMPERATURE SIMULATION

**Figure 29: Contour of Finish Rolling Temperature Field**

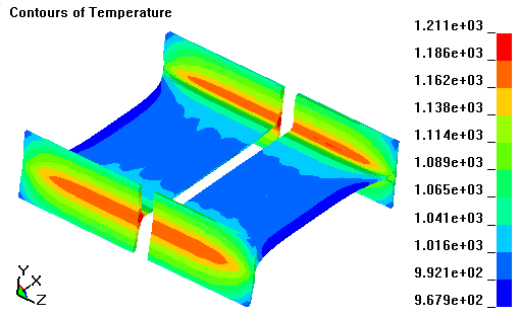


**Figure 30: xxxxxxxxxxxxxxxxxxxxxxx**

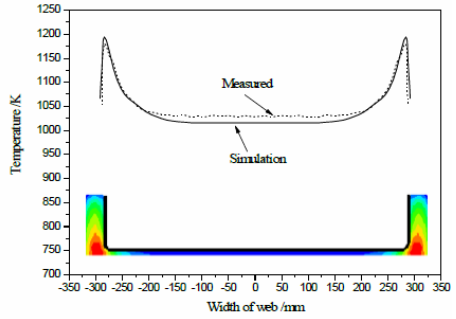


Fig. 6 Contour of the surface temperature large size H-Beam

Initial roll temperature- 313 K
Initial billet temperature- 1425 K
Friction Coefficient- 0.6

**Table 7: Temperature Variation from the centre of the beam to the end**

| Distance of the point from the centre (mm) | Temperature (K) |
|---|---|
| 0 | 0.697E+02 (MIN) |
| 50 | 0.721E+02 |
| 100 | 1.016E+03 |
| 150 | 1.041E+03 |
| 200 | 1.065E+03 |
| 250 | 1.211E+03(MAX) |

There are several factors that influence the temperature variation throughout the workpiece during H-Beam rolling. These factors includes: (1) The surface-to-volume ratio is different in various parts of workpiece. The web always has the highest surface-to-volume ratio, whereas in the flange it is relatively lower and the connection area of the web and flange has the lowest percentage. Because of that, the heat radiation status varied significantly in different parts of the section during rolling of the H-Beam. (2) The rolling temperature is relatively low. The surface area of workpiece which contacts to the roller, has an extremely drop of temperature, due to the heat conduction. (3) In the deformation zone the plastic work converts to the heat, so the temperature of some key points in the work piece has increased. (4) Because of the complexity of the H-Beam shape, the cooling water for the roller has accumulated in the tank space between both sides of flange. As a result, cooling water directly cools down the web, which is the main reason of the severely temperature difference in the section of large size H-beam. Figure 5 is the 3-D temperature contour of finish rolling. Figure 4.10 is the comparison of the temperature contour in the surface between simulation and measurement.

The comparison between simulated and measured results shows that the temperature field of the H-Beam can be simulated with good accuracy. It is clear that the temperature curve of different parts generally drops during the rolling process. In addition, there is a turning point, which drops sharply, in each pass of the rolling at the position that contacts with the roller. But the surface of the work piece turns to the higher temperature when the deformation occurs. At the same time, some inner points of the work piece in the deformation zone have an increase in the temperature curve. Temperature difference in various points that located inside of the work piece reduces as the work piece goes slim, whereas the temperature difference on the surface becomes more and more manifested.

## Variation of Moment (Mx) & Reaction Forces of the Top Roller

**Table 8: Variation of Moment of Top Roller**

| X component of the moment (Nm) | Time (sec) |
|---|---|
| 0 | 0.75 |
| 0 | 0.875 |
| -150 E+06 | 1 |
| -800 E+06 | 1.25 |
| -870 E+06 | 1.375 |
| -850 E+06 | 1.75 |

**Figure 30: Variation of Moment of Top Roller**

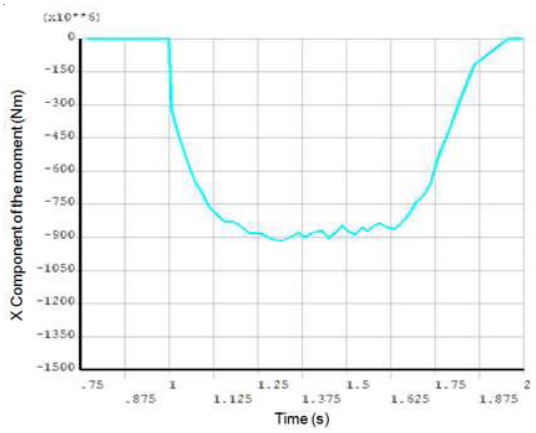


The plot suggests that rolling moment varies little from TIME = 1.25s to TIME = 1.6. The hot rolling process during this time range can be considered to be steady state.

**Table 9: Variation of Reaction Forces of Top Roller with Time**

| Time (sec) | Fx (N) | Fy (N) | Fz (N) |
|---|---|---|---|
| 0.75 | 0 | 0 | 0 |
| 0.875 | 0 | -500 E+06 | -300 E+06 |
| 1 | 150E+06 | -600 E+06 | -350 E+06 |
| 1.125 | 150 E+06 | -1500 E+06 | 250 E+06 |
| 1.25 | 200 E+06 | -1850 E+06 | 150 E+06 |
| 1.375 | 170 E+06 | -1900 E+06 | 110 E+06 |

**Figure 31: Variation of Reaction Forces of top Roller**

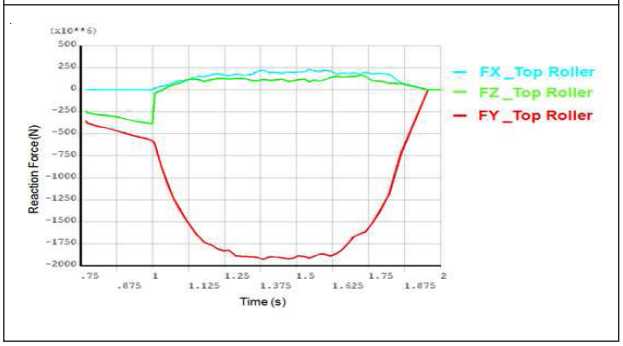


The plot also shows that forces vary little from TIME = 1.25 to TIME = 1.6s. As would be expected from the top roller, the Y component of the force (that is, the downward force) is dominant in the rolling process.

## Residual Stress Simulation

**Figure 32: Residual stress field of large H-Beam in the length direction**

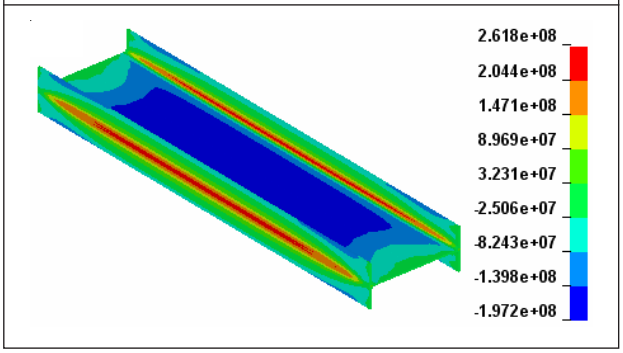


**Table 10: Variation of Residual Stress Along the Width of Beam**

| Distance from the centre (mm) | FEA Data (MPa) | Experimental (MPa) |
|---|---|---|
| 0 | 150 | 150 |
| 100 | 95 | 98 |
| 200 | 97 | 100 |
| 300 | 250 | 250 |

**Figure 33: Contrast of Residual Stress Between Simulation and Measurement**

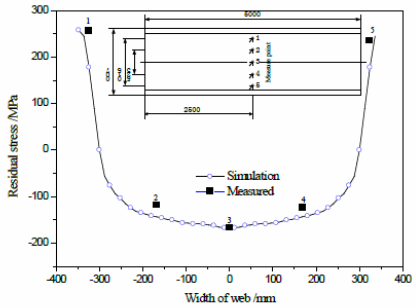


Figure 4.13 is the residual stress contour of large size H-Beam with the length of 3m after rolling. Figure 4.14 is comparison between the simulation and the measurement. Figure 13-14 shows that the stress status of entire web is compressive, whereas the connection area of the flange and web is tensile stress, and the top of the flange is also compressive stress. The highest stress value in the web occurs in symmetry center of the H-beam. The workpiece in this dimension has the highest residual stress of more than 160 MPa in the web and more than 250 MPa in the connection area of flange and web.

# CONCLUSION

A three-dimensional thermo-mechanical model of Hot rolling of structural seel is developed to simulate the hot rolling of A36 structural steel using finite element analysis software 'ANSYS v14.0'. To validate the FEA

model the values of temperature distribution and effective plastic strain rate during simulation are compared with the measured results and simulated results are found to be in good agreement with experimental results validating the model.

The simulation shows that

During the initial substep the element gets distorted. Thus, the solution gets diverged. Rezoning technique automatically creates the new mesh thereby improving the quality and allows the analysis to continue.

It is quite clear that the connection area of the flange and web experiences highest strain during rolling. For some duration in the rolling process, the plastic strain varies little over time in the high plastic strain region. This behavior occurs during the steady-state (rolling) phase of the simulation.

The stress contour in the pressing direction of horizontal roller during the rolling process, which shows that the highest stress is located in the connection area of flange and web during rolling.

The outer side of the flange flows toward top of the flange and the inner side of the flange flows toward the connection area of flange and web which is flow along the curve of horizontal roller. This reverse phenomenon shows that as an integrated work piece there is some sort of metal flow in the section of the H-beam in order to make up the difference of the stretching between the web and flange.

The temperature curve of different parts generally drops during the rolling process. In addition, there is a turning point, which drops sharply, in each pass of the rolling at the position that contacts with the roller. But the surface of the work piece turns to the higher temperature when the deformation occurs. At the same time, some inner points of the work piece in the deformation zone have an increase in the temperature curve. Temperature difference in various points that located inside of the work piece reduces as the work piece goes slim, whereas the temperature difference on the surface becomes more and more manifested.

The rolling moment varies little from TIME = 1.25s to TIME = 1.6. The hot rolling process during this time range can be considered to be steady state. The reaction forces vary little from TIME = 1.25 to TIME = 1.6s. As would be expected from the top roller, the Y component of the force (that is, the downward force) is dominant in the rolling process.

The stress status of entire web is compressive, whereas the connection area of the flange and web is tensile stress, and the top of the flange is also compressive stress. The highest stress value in the web occurs in symmetry center of the I-beam.

## REFERENCES

1. Asaro R J and Lubarda V A (2006), “Mechanics of Solids and Materials”, *Cambridge University Press, New York*, pp. 461-501.
2. Askenazi A and Adams V (1999), “Building Better Products with Finite Element Analysis”, *Onword Press, Santa Fe*, pp. 425-464.
3. Barrett C R, Nix W D and Tetelman, A S (1973), “The Principles of Engineering Materials”, *Prentice-Hall, Englewood Cliffs, New Jersey*,
4. Bathe K J and Wilson E L (1976), “Numerical Methods in Finite Element Analysis”, *Prentice Hall, N J*, pp. 82-83, 172-173, 176,184, 208, 246-249.
5. Bathe K J (1982), “Finite Element Procedures in Engineering Analysis”, *Prentice Hall, Englewood Cliffs, New*

*Jersey*, pp. 301-305, 407-418.

6. Belytschko T, Liu W K, and Moran B (2001), "Nonlinear Finite Elements for Continua and Structures", *John Wiley & Sons, Chichester*, pp. 570-580.
7. Birchenall C E (1959), "Physical Metallurgy", *McGraw Hill, New York*.
8. Brick R M, Pense A W and Gordon, R B, (1977), "Structure and Properties of Engineering Materials", *McGraw Hill, New York*.
9. Boresi A P and Chong K P (2000), "Elasticity in Engineering Mechanics", *2nd edition, John Wiley & Sons, New York*,
10. Boresi A P and Schmidt R J (2003), "Advanced Mechanics of Materials", *6th edition, John Wiley & Sons, New York*.
11. Burnett D S (1987), "Finite Element Analysis: from concepts to applications", *Addison Wesley Publishing, Menlo Park, California*.
12. Callister W D (1994) "Materials Science and Engineering - An Introduction", *3rd edition, John Wiley & Sons, New York*, pp. 149-153, 165-167, 349-350
13. Chadwick P (1999), "Continuum Mechanics: concise theory and problems", *Dover, New York*.
14. Champion E R (1992), "Finite Element Analysis in Manufacturing Engineering", *McGraw Hill, New York*, pp. 1-4
15. Christensen R M (1982), "Theory of Viscoelasticity", *2nd edition, Academic Press, New York*, pp. 90-94.
16. Cianci M (1999), "Leonardo da Vinci's Machines", *BecocciEditore, Florence*, pp. 89.
17. Clark D S (1962), "Physical Metallurgy for Engineers", *2nd edition, Van Nostrand, Princeton, New Jersey*.